Published in final edited form as:
J Neurol Sci. 2009 July 15; 282(1-2): 34–38. doi:10.1016/j.jns.2008.12.013.

Deep Gray Matter T2 Hypointensity Correlates with Disability in a Murine Model of MS

Istvan Pirko[a,*], **Aaron J. Johnson**[a], **Anne K. Lohrey**[a], **Yi Chen**[a], and **Jun Ying**[b]

[a]Department of Neurology, University of Cincinnati, 260 Stetson St, Cincinnati, OH 45267

[b]Department of Public Health Sciences, University of Cincinnati, 260 Stetson St, Cincinnati, OH 45267

Abstract

Advanced MRI studies demonstrated several diffuse non-lesional features in multiple sclerosis, including changes detectable in gray matter areas. Standard T2 weighted MRI scans of deep gray matter structures, including the thalamus, caudate, putamen, dentate nuclei often demonstrate hypointensity. T2 hypointensity has been shown to correlate with cognitive, neuropsychiatric and motor dysfunction. The exact pathogenesis of this MRI phenomenon remains unknown. In this manuscript, we demonstrate the first known MS animal model of deep gray matter T2 hypointensity. In TMEV infected SJL/J mice, gradual development of thalamic T2 hypointensity was noted over the disease course. Quantitative analysis of the hypointensity demonstrated a strong correlation between the degree of T2 hypointensity and rotarod detectable disability. We propose that this model will allow mechanistic studies investigating the pathogenesis and significance of deep gray matter T2 hypointensity in MS.

Keywords

T2 hypointensity; deep gray matter; iron deposition; EAE; TMEV; Theiler's murine encephalitis virus; multiple sclerosis; multiple sclerosis animal model; MS; MRI; magnetic resonance imaging

1. Introduction

Multiple sclerosis (MS) is an inflammatory demyelinating disease of the central nervous system (CNS). MS is the second most common cause of disability among young adults in their most productive years (1). The hallmark of MS is the lesion representing an area of inflammatory demyelination in the white matter of the brain, spinal cord, or the optic nerve(2). However, in addition to white matter lesions, gray matter areas are also known to be involved in MS, both from the standpoint of lesional(3) and non-lesional pathology(4). With the advent of advanced MRI studies, several non-lesional features of MS have been described; many of these serve as paraclinical disease markers(5). In general, they show a better association between clinical outcome measures than lesional MRI metrics(6). An important non-lesional feature of MS is

*Corresponding author: Istvan Pirko, MD, Associate Professor of Neurology, Director, Waddell Center for Multiple Sclerosis, 260 Stetson St, Suite 2300, Cincinnati, OH 45267-0525, Tel: 513 558 6503, Fax: 513 558 1434, Email: Istvan.Pirko@uc.edu.

the T2 hypointensity in deep gray nuclei(7,8). This hypointensity usually involves the thalamus and various basal ganglia nuclei. It has been demonstrated that T2 hypointensity has a close relationship with ambulatory and cognitive dysfunction and also with MRI detectable brain atrophy(9).

Cerebral gray matter T2 hypointensity is associated with disease duration, clinical course, and the level of disability in cross-sectional studies [7,8,21,22] and can predict both subsequent brain atrophy and progressive disability in longitudinal studies of MS [25]. In one study, Bakshi et al. demonstrated that globus pallidus hypointensity predicted T2 lesion load, whereas caudate hypointensity was the only variable associated with the EDSS score (10) on regression modeling comparing various MRI surrogates (8). In this study, T2 hypointensity of the thalamus, caudate, and putamen differentiated the secondary progressive from the relapsing-remitting clinical courses. A study by the same investigators of 47 MS patients and 15 healthy controls established that dentate T2 hypointensity was the only MRI variable significantly correlated with 25 foot timed walk, a commonly used disability measure. It was also the best MRI correlate of physical disability (EDSS) score in regression modeling in this cohort (11). In a recent study conducted at 3 Tesla by another group, a significant correlation between the EDSS and signal intensity in the globus pallidus and the caudate nucleus was demonstrated (12). In addition to physical disability, excessive gray matter iron deposition as estimated by MRI also correlates well with cognitive dysfunction, as demonstrated by two groups of investigators (13).

Very little is known about the influence of disease modifying therapies on T2 hypointensity. Bermel et al demonstrated that interferon β-1a treatment may modify T2 hypointensity related disease outcomes in a favorable way. In the original IM interferon β-1a study, T2 hypointensity was chosen in regression modeling as the best predictor of atrophy at the one and 2-year time points in placebo treated patients. In the interferon group, no relationship existed between baseline T2 hypointensity and atrophy (14).

The hypointense areas are thought to represent iron deposition as suggested by recent advanced MRI studies utilizing magnetic field correlation or phase imaging techniques (15) although histologic-MRI correlation data providing proof of link to excessive iron are limited in this regard(16). From the MRI standpoint, a variety of factors that give rise to susceptibility effects can result in T2 hypointensity. These factors include but are not limited to iron or other paramagnetic metals, free radicals, and the presence of macrophages [9]. Regardless of its cause, gray matter T2 hypointensity is clearly related to relevant clinical features in MS. Therefore, it would be critically important to determine the pathogenesis leading to the development of this imaging finding.

Animal MS models manifesting T2 hypointensity would allow for mechanistic investigations of the pathogenesis of gray matter T2 hypointensity. Such models could lay the groundwork for the development of therapeutic strategies addressing this important feature of MS. However, while excessive CNS iron deposition has been linked to the pathophysiology animal models of MS(17–21), the presence of T2 hypointensity has not yet been investigated in these models. Although experimental allergic encephalomyelitis (EAE) remains the most commonly studied MS model in mice, and EAE-based research has made seminal contributions to our understanding of CNS inflammation (22), recent publications highlight the relevance of alternative models (23–25). Theiler's Murine Encephalitis Virus (TMEV) is the most frequently used infection induced model of MS(26). In susceptible mouse strains, intracranial TMEV infection follows a biphasic pattern: the first stage is charecterized by a transient meningo-encephalitis, which completely recovers in approximately 2–3 weeks. The second stage is the chronic demyelinating stage, with associated progressively worsening disability. Susceptibility to this late demyelinating stage is determined by MHC class I molecules, and

the main mediators of pathology are most likely CD8 T cells and macrophages. There is viral persistence in the demyelinating stage, but epitope spread to myelin epitopes has also been demonstrated(27). In this study, we demonstrate that T2 hypointensity of thalamic nuclei are present in a Theiler's Murine Encephalitis Virus (TMEV) induced murine model of MS. TMEV. Similarly to MS, this imaging finding correlates well with disability in our newly established mouse model.

2. Materials and Methods

2.1 Mice

SJL/J mice were purchased from the Jackson Laboratory (Bar Harbor, ME). All the experiments were approved by the Institutional Animal Care and Use Committee at the University of Cincinnati, and all the animals were housed according to established institutional guidelines. 8 TMEV infected and 6 age matched non-infected control mice (control group) were followed in this experiment. MRI scans were performed for all mice repeatedly at 1, 4, 6 and 12 months after disease induction were acquired and analyzed. Disability was monitored with the rotarod assay, performed at the same time points, within 2 days before or after MRI scans.

2.2 Theiler's Virus Infection

TMEV infection was produced by intracerebral virus injection of 9 week old mice anesthetized with inhalational isoflurane. With a 27-gauge needle attached to a Hamilton syringe, 10 μL volume containing 200,000 PFU purified Daniel's strain of TMEV was injected intracerebrally resulting in 99% incidence of infection. TMEV infection in susceptible strains is followed by an inflammatory demyelinating disease, and serves as an accepted MS model(26,28).

2.3 Rotarod assay

Once every month, the animals' motor ability was assessed using the Rotamex-5 rotarod apparatus (Columbus Instruments, Columbus, Ohio). The apparatus consists of a rotating rod, on which the animals are trained to march. The RPM of the rod is increased at a constant rate from 5–40 over 7 minutes. Eventually, the animals are no longer able to negotiate the rotating rod and fall. The time spent on the rotating rod is recorded by the device, and serves as numerical data for our analysis. At each time point, the animals are measured twice on the same day and their best performance is recorded. In addition, the animals are trained on the rotarod for a month prior to disease induction, in order to minimize the impact of motor learning on our experiments.

2.4 Magnetic resonance imaging (MRI)

Image acquisition was performed as described earlier in a Bruker Biospec 300 MHz (7 Tesla) horizontal bore small animal imaging system (Bruker Biospin, Billercia, MA) equipped with probes and custom-built coils for mouse brain imaging(29,30). The ~37 °C core temperature of the animals was maintained by a thermocouple based system using a circulating hot water heater embedded in the probes. Inhalational isoflurane anesthesia (1.75% in room air) was delivered via a nose cone. The animals were constantly monitored by ECG and respiratory rate using an MRI compatible monitoring and gating system (SA Instruments, Inc.; Stony Brook, NY). A respiratory gated T2 weighted volume acquisition RARE sequence was used for in vivo MRI acquisition (spin echo-based RARE sequence, TR: 1500ms, TE: 70ms, RARE factor: 16, FOV: 3. 20×1.92×1.92 cm, matrix: 256×128×128). By using 3D datasets, we are able to generate arbitrarily oriented slices. For on-site image monitoring, we used Bruker's Xtip Image.

2.5 MRI postprocessing, including coregistration, slice extraction and intensity analysis

All 3D images were co-registered to a base image using a 6 degree of freedom rigid body registration algorithm in the 3D Voxel Registration module of Analyze, a standard biomedical image analysis software (Analyze 8.1; Mayo Clinic Biomedical Imaging Resource, Rochester, MN)(31,32)). The Region of Interest Tool was then used to extract a standard coronal slice from the 3D dataset. To measure intensity, a square region of interest (2×2 pixels) was drawn in the thalamus using the ROI analysis tool in Analyze. Measurements of intensity were taken in two regions, the lateral nucleus and the medio-dorsal nucleus (Fig. 1). Intensity from an identical sized ROI placed in the ventricular cerebrospinal fluid (CSF) was also taken for each subject as a method of intensity normalization. The adjusted intensity by taking ratios of the lateral nucleus and/or the medio-dorsal nucleus to the CSF background was used as the outcome measure (referred to as MEAS/CSF ratio in our study). The normalization for intensity differences across scans is necessary due to varying scanner calibration and shimming between the acquisitions.

3. Statistical analysis

MEAS/CSF ratios and the rotarod score were summarized by mean ± standard error (SE). Mixed effect models were used to assess associations of numerical measures to the time effect (months 1, 4, 6 and 12) and the treatment effect (experiment vs. control), using a random effect (individual mice) to account for within subject correlation caused by repeated observations. *Post hoc* comparisons of means longitudinally between months in each group and cross sectionally between groups at each month were performed under the mixed effect model framework and adjusted for overall type 1 error using Tukey's multiple comparison methods. Relationships between the rotarod score and the MRI measures were assessed using linear models, using a random effect to account for within subject correlation. Finally, intra-class correlations (ICC's) were used to assess agreements of MRI measures between the two thalamic areas assessed in the study (VM and L thalamus). All statistical analyses were performed using a SAS 9.1 software (SAS, Cary, NC) package. P-values <0.05 were considered statistically significant. The agreement was considered "excellent", "substantial", "very good", "good", "fair", and "poor" if the ICC was 90–100%, 80–89%, 70–79%, 60–69%, and 50–59%, and <50% respectively.

4. Results

In this study, we analyzed the intensity of two thalamic nuclei: the medio-dorsal and the lateral nucleus complex of the thalamus. We chose these areas since they showed obvious changes, including incremental changes associated with the disease course, on overall visual inspection of the MRI images. Examples of the time course and of the appearance of these nuclei are shown on Fig. 2.

A total of 14 mice, 8 in the experiment group and 6 in the control group were studied. Mice in the experimental group showed a progressive T2 hypointensity after month 4, while those in the control group showed no significant change over the time. In case of the medio-dorsal thalamic nucleus, even at the 1 month time point we already found significant differences. The rotarod score was also decreased in the experimental group after month 4, consistent with the animals' worsening disability (Table 1 and Fig. 3 A–C). The normalized intensity measurements showed positive relationships to the rotarod score in the medial thalamic area among infected mice, indicating a link between T2 hypointensity and disability (Table 2 and Fig. 3 D). Similar results were obtained measuring intensities in the lateral thalamic area. The agreement between the medial and lateral thalamic area measurements was very good with ICC-s of 79% for the two normalized intensity values.

5. Discussion

Our results clearly establish that deep gray matter hypointensity is present in this murine MS model, and that thalamic hypointensity shows a strong correlation with rotarod detectable disability. Our experiments have not yet involved MRI-tissue correlation analysis. However, the model will clearly allow for investigations of this phenomenon at the tissue level. In addition to extracellular iron deposition, the presence of deoxyhemoglobin, macrophages or free radicals may also give rise to T2 hypointensity. The model will allow us to determine the main contributors to the physical phenomenon of T2 hypointensity in CNS inflammation. In human MS, such studies can only be conducted in autopsy material, as deep gray matter biopsy, especially thalamic biopsy would virtually never be performed in MS cases. Since the initial description of this phenomenon is relatively recent, correlative autopsy studies are very few in MS(16).

While there are no current papers investigating T2 hypointensities in animal models, iron deposition has been implicated as playing a role in EAE-based models, as mentioned earlier. In a spinal cord homogenate-complete Freud's adjuvant (CFA) induced EAE model in SJL mice, iron deposits were found in the preclinical stage, and also in the recovery stage to a lesser extent(18). It is suspected that this finding may represent extravasated blood, which is known to occur in this model(18). In addition, it was demonstrated that iron chelating agents can dramatically suppress the severity and duration of EAE in rats induced by spinal cord homogenates and CFA. This suggests a strong role for iron in the regulation of this disease model (33). Another study established that the effects of iron chelation are likely acting on the afferent limb of the immune response to spinal cord homogenate (34). In this model, extensive lipid breakdown needs to occur before adequate antigen presentation can take place, and it is at this level that iron chelation exerts its inhibitory effect. More recently, the clinical signs of EAE were significantly reduced with iron chelation in an MBP induced EAE model (19). Effects of iron chelation have never been reported in viral or toxin-induced models of MS.

Gray matter features of MS are getting increasing attention in the MS literature (4). It has been demonstrated in several studies that cortical and subcortical gray matter pathology is detectable in MS. These findings are present at an early stage, including even in clinically isolated syndromes that later convert to MS. Thalamic pathology, including atrophy, T2 hypointensity of thalamic nuclei and abnormalities on advanced MRI scans have been demonstrated in MS (35–38). The connection between these MRI findings and their relationship to an as of yet poorly defined underlying pathomechanism remains an active area of MS research. We believe that our model may represent an additional pathway towards a more complete understanding of the neurodegenerative component in MS.

With the completion of our proof-of-principle study, we also plan to determine the temporal characteristics of T2 hypointensity in other deep gray nuclei that have been found relevant in MS, including the caudate, putamen, red nucleus, and dentate nucleus (8,11). In addition, we plan to investigate this phenomenon in other TMEV susceptible mouse strains. In case interstrain differences are found, that would enable us to understand potential genetic determinants of T2 hypointensities. Since our model is induced by a viral infection, we will also need to determine the specific viral loads in the deep gray nuclei in question. Of note, while in the early stage of TMEV infection neurons are thought to be infected (in the deep gray matter as well), in the late demyelinating stage including the time points in our study, neurons are no longer thought to be carriers of the virus (28). In the late stages, epitope spread was reported to occur, with the immune cells addressing myelin-derived as opposed to viral epitopes (27). The relevance of epitope spread in our model remains to be investigated. A limitation of the current study is that spin echo-based sequences were used, whereas gradient echo-based

sequences are more sensitive to the susceptibility effects caused by iron deposition. In future extensions of this project, both sequences will be utilized and compared.

We propose that our newly established T2 hypointensity model may serve as a fertile ground for future research into the role and significance of this novel MS-related MRI finding. Since T2 hypointensity shows strong correlation with disease severity measures, our model may help us gain insight into the substrate of disability in MS.

References

1. Noseworthy JH, Lucchinetti C, Rodriguez M, Weinshenker BG. Multiple sclerosis. N Engl J Med 2000;343(13):938–952. [PubMed: 11006371]
2. Lucchinetti CF, Parisi J, Bruck W. The pathology of multiple sclerosis. Neurol Clin 2005;23(1):77–105. [PubMed: 15661089]vi.
3. Kutzelnigg A, Lassmann H. Cortical lesions and brain atrophy in MS. J Neurol Sci 2005;233(1–2): 55–59. [PubMed: 15893328]
4. Pirko I, Lucchinetti CF, Sriram S, Bakshi R. Gray matter involvement in multiple sclerosis. Neurology 2007;68(9):634–642. [PubMed: 17325269]
5. Zivadinov R, Cox JL. Neuroimaging in multiple sclerosis. Int Rev Neurobiol 2007;79:449–474. [PubMed: 17531854]
6. Zivadinov R, Leist TP. Clinical-magnetic resonance imaging correlations in multiple sclerosis. J Neuroimaging 2005;15(4 Suppl):10S–21S. [PubMed: 16385015]
7. Bakshi R, Dmochowski J, Shaikh ZA, Jacobs L. Gray matter T2 hypointensity is related to plaques and atrophy in the brains of multiple sclerosis patients. J Neurol Sci 2001;185(1):19–26. [PubMed: 11266686]
8. Bakshi R, Benedict RH, Bermel RA, Caruthers SD, Puli SR, Tjoa CW, et al. T2 hypointensity in the deep gray matter of patients with multiple sclerosis: a quantitative magnetic resonance imaging study. Arch Neurol 2002;59(1):62–68. [PubMed: 11790232]
9. Neema M, Stankiewicz J, Arora A, Dandamudi VS, Batt CE, Guss ZD, et al. T1- and T2-based MRI measures of diffuse gray matter and white matter damage in patients with multiple sclerosis. J Neuroimaging 2007;17:16S–21S. [PubMed: 17425729]
10. Kurtzke JF. Historical and clinical perspectives of the Expanded Disability Status Scale. Neuroepidemiology 2008;31(1):1–9. [PubMed: 18535394]
11. Tjoa CW, Benedict RH, Weinstock-Guttman B, Fabiano AJ, Bakshi R. MRI T2 hypointensity of the dentate nucleus is related to ambulatory impairment in multiple sclerosis. J Neurol Sci 2005;234(1–2):17–24. [PubMed: 15993137]
12. Zhang Y, Zabad RK, Wei X, Metz LM, Hill MD, Mitchell JR. Deep grey matter "black T2" on 3 tesla magnetic resonance imaging correlates with disability in multiple sclerosis. Mult Scler 2007;13(7): 880–883. [PubMed: 17468444]
13. Brass SD, Benedict RH, Weinstock-Guttman B, Munschauer F, Bakshi R. Cognitive impairment is associated with subcortical magnetic resonance imaging grey matter T2 hypointensity in multiple sclerosis. Mult Scler 2006;12(4):437–444. [PubMed: 16900757]
14. Bermel RA, Puli SR, Rudick RA, Weinstock-Guttman B, Fisher E, Munschauer FE 3rd, et al. Prediction of longitudinal brain atrophy in multiple sclerosis by gray matter magnetic resonance imaging T2 hypointensity. Arch Neurol 2005;62(9):1371–1376. [PubMed: 16157744]
15. Ge Y, Jensen JH, Lu H, Helpern JA, Miles L, Inglese M, et al. Quantitative assessment of iron accumulation in the deep gray matter of multiple sclerosis by magnetic field correlation imaging. AJNR Am J Neuroradiol 2007;28(9):1639–1644. [PubMed: 17893225]
16. Drayer B, Burger P, Hurwitz B, Dawson D, Cain J. Reduced signal intensity on MR images of thalamus and putamen in multiple sclerosis: increased iron content? AJR Am J Roentgenol 1987;149 (2):357–363. [PubMed: 3496764]
17. Levine SM, Chakrabarty A. The role of iron in the pathogenesis of experimental allergic encephalomyelitis and multiple sclerosis. Ann N Y Acad Sci 2004;1012:252–266. [PubMed: 15105271]

18. Forge JK, Pedchenko TV, LeVine SM. Iron deposits in the central nervous system of SJL mice with experimental allergic encephalomyelitis. Life Sci 1998;63(25):2271–2284. [PubMed: 9870713]
19. Pedchenko TV, LeVine SM. Desferrioxamine suppresses experimental allergic encephalomyelitis induced by MBP in SJL mice. J Neuroimmunol 1998;84(2):188–197. [PubMed: 9628462]
20. Grant SM, Wiesinger JA, Beard JL, Cantorna MT. Iron-deficient mice fail to develop autoimmune encephalomyelitis. J Nutr 2003;133(8):2635–2638. [PubMed: 12888650]
21. Mitchell KM, Dotson AL, Cool KM, Chakrabarty A, Benedict SH, LeVine SM. Deferiprone, an orally deliverable iron chelator, ameliorates experimental autoimmune encephalomyelitis. Mult Scler 2007;13(9):1118–1126. [PubMed: 17967839]
22. Steinman L, Zamvil SS. How to successfully apply animal studies in experimental allergic encephalomyelitis to research on multiple sclerosis. Ann Neurol 2006;60(1):12–21. [PubMed: 16802293]
23. Lassmann H, Ransohoff RM. The CD4-Th1 model for multiple sclerosis: a critical [correction of crucial] re-appraisal. Trends Immunol 2004;25(3):132–137. [PubMed: 15036040]
24. Sriram S, Steiner I. Experimental allergic encephalomyelitis: a misleading model of multiple sclerosis. Ann Neurol 2005;58(6):939–945. [PubMed: 16315280]
25. Nelson AL, Bieber AJ, Rodriguez M. Contrasting murine models of MS. Int MS J 2004;11(3):95–99. [PubMed: 15585167]
26. Rodriguez M, Oleszak E, Leibowitz J. Theiler's murine encephalomyelitis: a model of demyelination and persistence of virus. Crit Rev Immunol 1987;7(4):325–365. [PubMed: 2827957]
27. Katz-Levy Y, Neville KL, Girvin AM, Vanderlugt CL, Pope JG, Tan LJ, et al. Endogenous presentation of self myelin epitopes by CNS-resident APCs in Theiler's virus-infected mice. J Clin Invest 1999;104(5):599–610. [PubMed: 10487774]
28. Brahic M. Theiler's virus infection of the mouse, or: of the importance of studying animal models. Virology 2002;301(1):1–5. [PubMed: 12359440]
29. Pirko I, Nolan TK, Holland SK, Johnson AJ. Multiple sclerosis: pathogenesis and MR imaging features of T1 hypointensities in a [corrected] murine model. Radiology 2008;246(3):790–795. [PubMed: 18309014]
30. Pirko I, Fricke ST, Johnson AJ, Rodriguez M, Macura SI. Magnetic resonance imaging, microscopy, and spectroscopy of the central nervous system in experimental animals. NeuroRx 2005;2(2):250–264. [PubMed: 15897949]
31. Robb RA. The biomedical imaging resource at Mayo Clinic. IEEE Trans Med Imaging 2001;20(9):854–867. [PubMed: 11585203]
32. Robb RA. 3-D visualization in biomedical applications. Annu Rev Biomed Eng 1999;1:377–399. [PubMed: 11701494]
33. Bowern N, Ramshaw IA, Clark IA, Doherty PC. Inhibition of autoimmune neuropathological process by treatment with an iron-chelating agent. J Exp Med 1984;160(5):1532–1543. [PubMed: 6333485]
34. Willenborg DO, Bowern NA, Danta G, Doherty PC. Inhibition of allergic encephalomyelitis by the iron chelating agent desferrioxamine: differential effect depending on type of sensitizing encephalitogen. J Neuroimmunol 1988;17(2):127–135. [PubMed: 2447124]
35. Wylezinska M, Cifelli A, Jezzard P, Palace J, Alecci M, Matthews PM. Thalamic neurodegeneration in relapsing-remitting multiple sclerosis. Neurology 2003;60(12):1949–1954. [PubMed: 12821738]
36. Cifelli A, Arridge M, Jezzard P, Esiri MM, Palace J, Matthews PM. Thalamic neurodegeneration in multiple sclerosis. Ann Neurol 2002;52(5):650–653. [PubMed: 12402265]
37. Fabiano AJ, Sharma J, Weinstock-Guttman B, Munschauer FE 3rd, Benedict RH, Zivadinov R, et al. Thalamic involvement in multiple sclerosis: a diffusion-weighted magnetic resonance imaging study. J Neuroimaging 2003;13(4):307–314. [PubMed: 14569822]
38. Houtchens MK, Benedict RH, Killiany R, Sharma J, Jaisani Z, Singh B, et al. Thalamic atrophy and cognition in multiple sclerosis. Neurology 2007;69(12):1213–1233. [PubMed: 17875909]

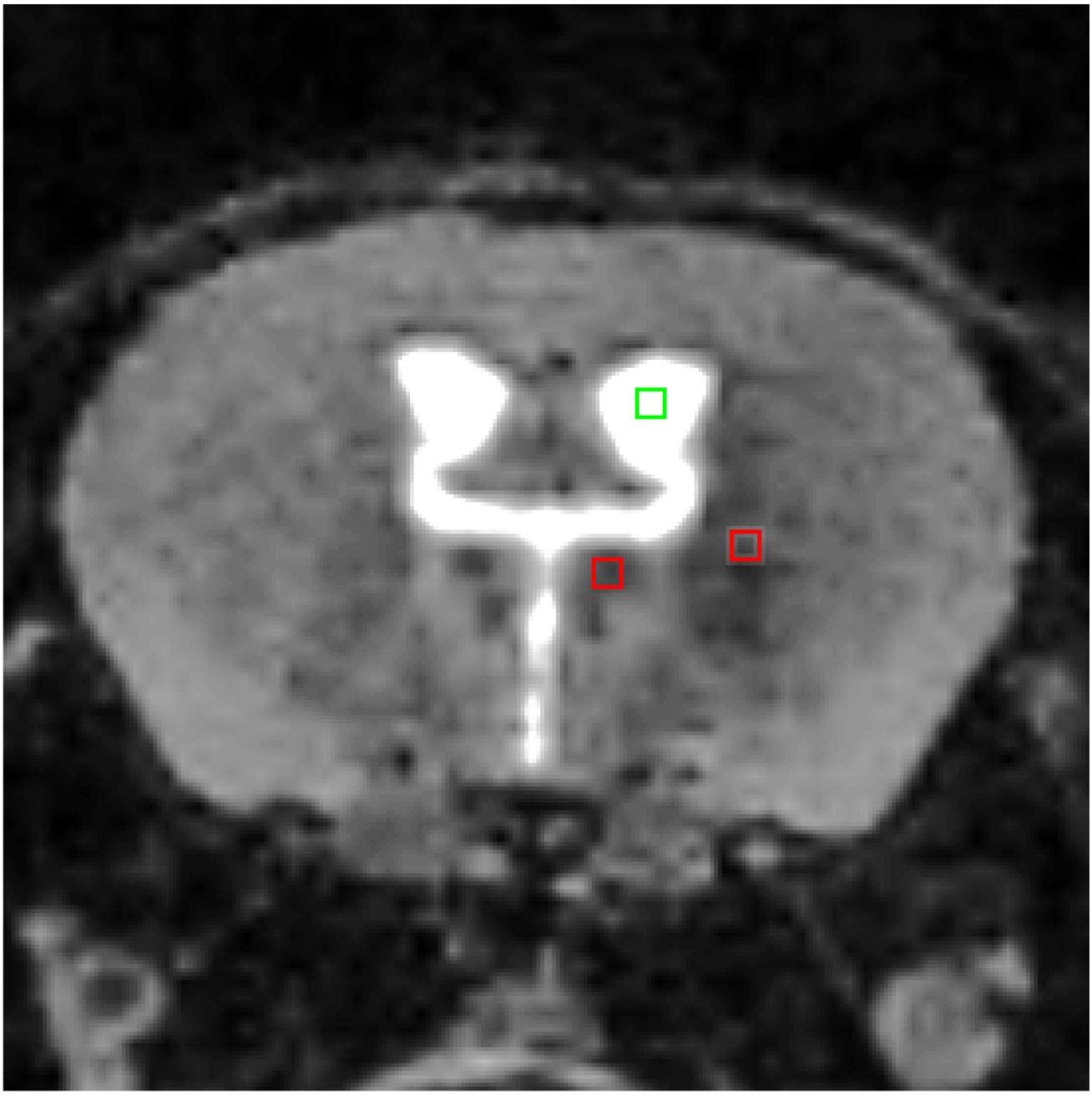

Fig. 1. Technique of hypointensity measurement

The above coronal MRI image shows an example of the 3 measurement points utilized in the generation of our data. The intensity values represented in the green frame were measured in Analyze 8.1, and served as the CSF intensity value. The two red frames show the location of the measured medial and lateral thalamic nuclei. The slices were extracted from co-registered 3D datasets. Therefore, the sampling of the studied areas of interest was conducted as closely as possible on slices representing the same brain areas across the datasets.

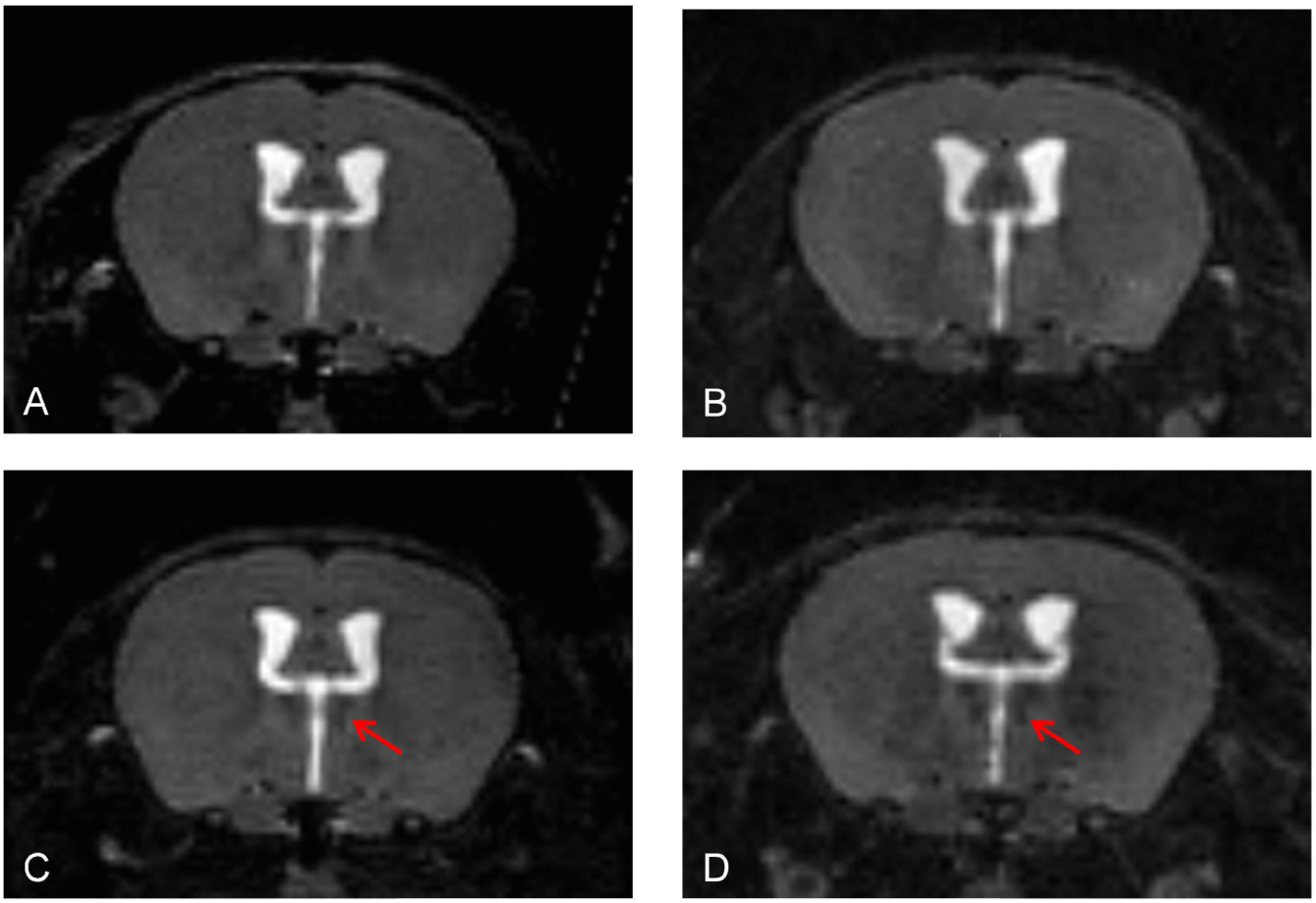

Fig. 2. Example of progressive thalamic T2 hypointensity at 1 (A), 4 (B), 6(C) and 12 (D) months post disease induction

A–D represent coronal slices of the section where the hypointensity was measured, as shown on Figure 1. The above images were extracted from the original 3D datasets. Note the hypointensity of the medio-dorsal thalamic nucleus and the increasing hypointensity at the later time points (arrows).

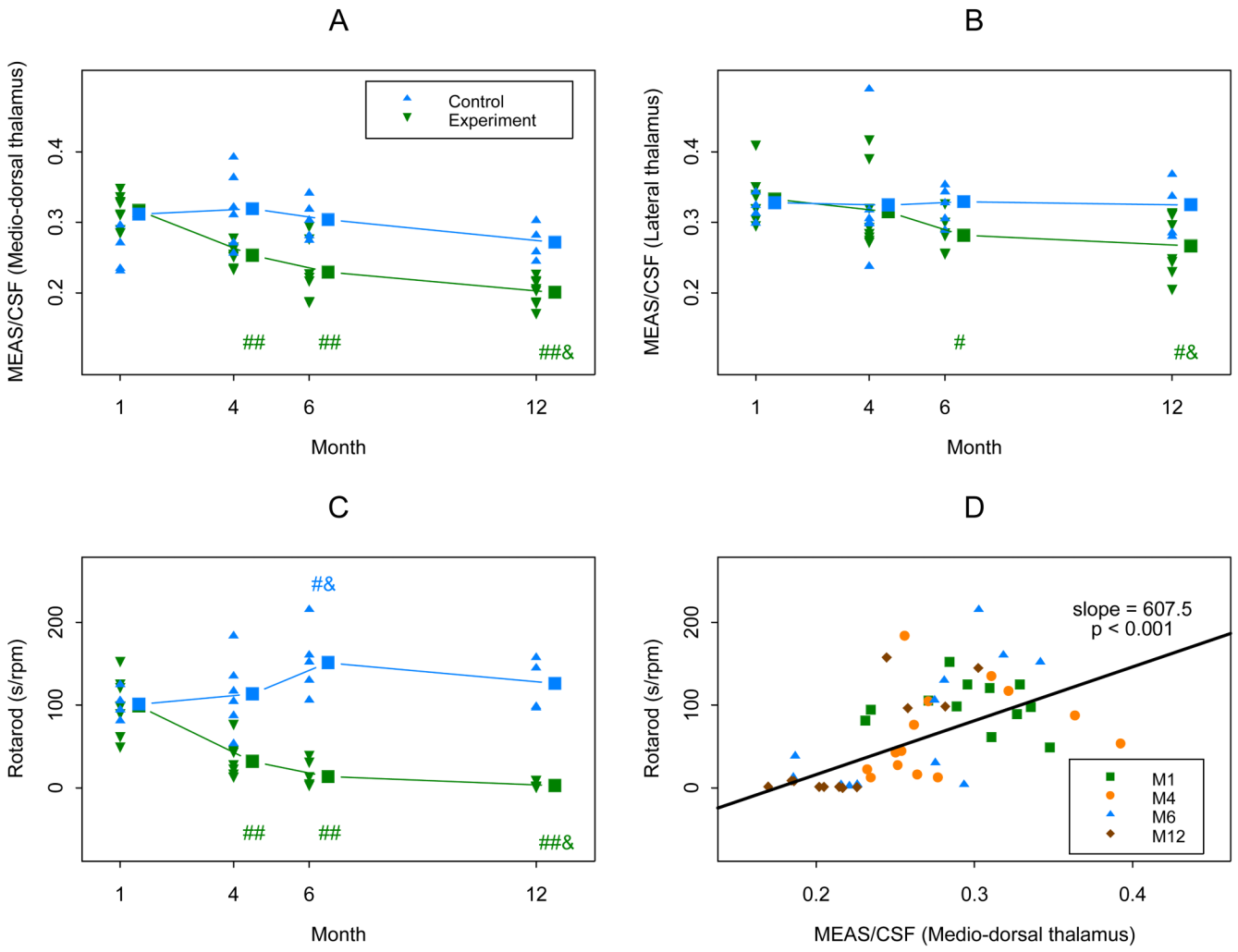

Fig. 3. Plots of MRI measures and rotarod measure

In plots (A)–(C), triangle dots in blue and reversed triangle dots in green indicate real observations from the control group and the experiment groups respectively. "##" and "#" in green indicate the mean of the experiment group in the follow up month (4, or 6, or 12) is significantly decreased from that of month 1, with $p<0.01$ and 0.05 respectively; and a "&" in green indicates the mean of month 12 is lower than that of month 4 with $p<0.05$ in the experiment group. A "#" and a "&" in blue indicate the mean of month 6 is higher than those of months 1 and 4 respectively with $p<0.05$ in the control group.

In plot (D), the slope was estimated using a mixed linear model using a random effect to account for within subject (mouse) correlation caused by repeated observations. The $p<0.001$ suggests the positive relationship between the Rotarod measure and the MEAS/FSA ratio using Medio-dorsal thalamus. M1, M4, M6, and M12 indicate observations at months 1, 4, 6 and 12 respectively.

Table 1

Summary of ROTAROD and MRI findings by month

	MEAS / CSF ratio								
	Medio-dorsal thalamus			Lateral thalamus			Rotarod score (seconds)		
Month	**E**†	**C**†	**p (E-C)**‡	**E**†	**C**†	**p (E-C)**‡	**E**†	**C**†	**p (E-C)**‡
1	0.32 (0.03)	0.32 (0.04)	0.956	0.33 (0.02)	0.32 (0.05)	0.652	99.05 ± 9.95	101.23 ± 14.10	0.901
4	0.25 (0.04) ##	0.32 (0.05)	<0.001	0.31 (0.07)	0.32 (0.05)	0.709	31.90 ± 9.95 ##	113.46 ± 11.51	<0.001
6	0.23 (0.06) ##	0.30 (0.05)	<0.001	0.28 (0.04) #	0.33 (0.08)	0.097	13.71 ± 10.61##	151.23 ± 12.59 #&	<0.001
12	0.20 (0.03) ##&	0.27 (0.04)	<0.001	0.27 (0.04) #&	0.32 (0.05)	0.056	2.96 ± 9.92##&	126.29 ± 14.04	<0.001

†Values in cells are mean (standard deviation), values after ± are SEM; E = experiment group; and C = control group.

‡p<0.05 indicates a significant difference of means between the groups.

"#" and "##" indicate the mean of month 4, or 6 or 12 is different from that of month 1, with p<0.05 and 0.01 respectively; and a "&" indicates the mean of month 6 or 12 is different from that of month 4, with p<0.05.

J Neurol Sci. Author manuscript; available in PMC 2010 July 15.

Table 2

Summary of relationship between rotarod score and MEAS / CSF ratio

MEAS/CSF ratio	Group[†]	Slope[‡]	p[§]
Medio-dorsal thalamus	E	607.5 ± 113.9	<0.001
	C	−53.1 ± 193.1	0.790
	E-C	660.7 ± 229.2	0.005
Lateral thalamus	E	390.3 ± 152.8	0.019
	C	−56.1 ± 193.8	0.779
	E-C	446.5 ± 240.4	0.047

[†] E = experiment group; C = control group; E-C = difference (of slopes) between experiment and control groups.

[‡] Values in cells are mean ± standard error (or SE) of slope parameters estimated from mixed linear models.

[§] A $p<0.05$ indicates the slope > 0 (or <0) significantly, or the significantly positive (or negative) relationship between the ROTAROD score and the corresponding MRI measure.